This is the accepted manuscript version of the final work appeared in *Environmental Science: Water Research & Technology* that has gone through peer-reviewed and technical editing. To access the final edited and published work, please see https://doi.org/10.1039/D0EW01007C

Effects of Peracetic Acid on Aromatic Polyamide Nanofiltration Membranes: A Comparative Study with Chlorine

Mohsen Ghafari[1], Tashfia M. Mohona[1], Lei Su[1], Haiqing Lin[2], Desiree L. Plata[3], Boya Xiong[3,4*], Ning Dai[1*]

[1]Department of Civil, Structural and Environmental Engineering, University at Buffalo, The State University of New York, Buffalo, NY 14260

[2]Department of Chemical and Biological Engineering, University at Buffalo, The State University of New York, Buffalo, NY 14260

[3]Department of Civil and Environmental Engineering, Massachusetts Institute of Technology, Cambridge, MA 02139

[4]Department of Civil, Environmental and Geo- Engineering, University of Minnesota, Minneapolis, MN 55455

* Corresponding authors:

Ning Dai: Email: ningdai@buffalo.edu. Phone: 716-645-4015. Address: 231 Jarvis Hall, Buffalo, NY 14260, USA.

Boya Xiong: Email: bxiong@umn.edu. Address: 500 Pillsbury Dr. SE, Minneapolis, MN 55455, USA.

Abstract

Peracetic acid (PAA) is being considered as a disinfectant in membrane-based wastewater reuse systems, but its compatibility with polyamide membranes has not been thoroughly investigated. In this work, we showed that PAA induced much less change in the performance and material characteristics of NF90 membranes than the traditional disinfectant free chlorine (NaOCl). The change in membrane water flux and the rejection of salt and neutral organic compounds after PAA exposure (1–180 g h L^{-1}) is significantly less than that resulted from NaOCl exposure at levels as low as 1 g h L^{-1}. The presence of two wastewater constituents, chloride or Fe(II), did not have significantly impact membrane performance upon exposure to PAA. Surface characterization showed that oxygen was incorporated into polyamide by PAA, some of which was attributed to the formation of carboxylic acid groups. Experiments using a model aromatic amide, benzanilide, indicated an unexpected role of PAA in protecting membrane from radicals formed by Fe(II) and the H_2O_2 present in commercial PAA formulations. Furthermore, product identification suggests that both amide bond breakage and ring oxidation are possible reaction mechanisms for PAA. Our findings support that PAA is a viable disinfectant candidate for wastewater reuse and warrants further evaluation.

TOC Art

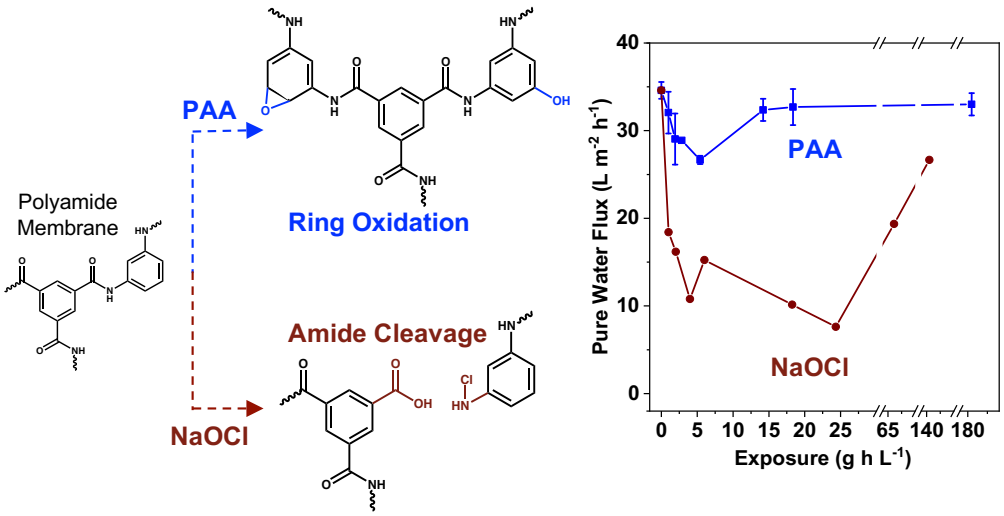

Keywords

Polyamide membrane, Membrane stability, Peracetic acid, Benzanilide, Wastewater reuse

1 Introduction

Aromatic polyamide thin-film composite membranes are widely used in reverse osmosis (RO) and nanofiltration (NF) in advanced treatment systems for potable reuse of wastewater.[1, 2] Biofouling remains one of the biggest operational challenges for these membrane systems.[3] The conventional disinfectant free chlorine (i.e., hypochlorous acid and hypochlorite) is effective in suppressing microbial growth, but it also degrades the crosslinked polyamide active layer, in a process initiated by *N*-chlorination followed by hydrolysis or ring chlorination via Orton rearrangement.[4, 5] In fact, most commercial polyamide membranes have a strict free chlorine tolerance limit as low as 0.1 mg L^{-1}.[6] As a result, many membrane-based potable reuse systems use the weaker disinfectant chloramine in RO pretreatment.[7-9] Additionally, concerns have been raised for the carcinogenic disinfection byproducts formed by the reactions between free/combined chlorine and wastewater organic matter, many of which are poorly rejected by RO membranes.[9, 10] To date, most research efforts focus on modifying membrane surfaces to prevent biofouling or modifying the synthesis procedures of polyamide membranes to increase their chlorine tolerance.[11-14] In comparison, less effort has been made to explore alternative disinfectants that are capable of controlling biofouling without damaging the polyamide active layer. Hydrogen peroxide (H_2O_2), despite being commonly used for membrane cleaning and exhibiting good polyamide compatibility,[15-17] is a weak disinfectant.[18] The other alternative disinfectants that have been investigated are primarily organic chloramines.[19, 20]

Peracetic acid (PAA) is an organic peroxide disinfectant being considered for wastewater disinfection. Commercial PAA mixtures contain PAA, H_2O_2, and acetic acid, where the latter two are present to minimize PAA hydrolysis (reaction 1). The mass ratio of PAA to H_2O_2 varies among commercial formulations, but 1:1.5 is common.[21] Laboratory- and pilot-scale wastewater disinfection studies showed that PAA can achieve inactivation of

suspended indicator bacteria similar to chlorine.[18, 22-25] Moreover, biofilm studies showed that PAA was comparable with or better than chlorine at reducing the viable cell counts of *Staphylococcus aureus* and *Pseudomonas aeruginosa* in their respective biofilms[26] and preventing the regrowth of planktonic and biofilm cells of *P. aeruginosa* and *Bacillus* sp. in the presence of organic matter.[27] PAA forms aldehydes as disinfection byproducts, but it forms much less carcinogenic halogenated byproducts than chlorine.[28] The presence of H_2O_2 in commercial PAA formulations can further minimize the formation of halogenated disinfection byproducts.[29]

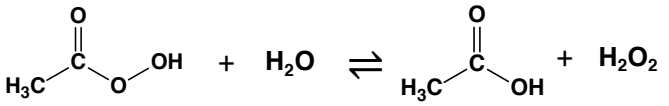

(R1) $K = 0.48–0.96$ [29]

PAA is an approved membrane cleaning reagent[6] and has been demonstrated to prevent biofouling in industrial RO systems,[30] but its reaction with polyamide has not been thoroughly investigated under conditions relevant to wastewater reuse systems. The potential interaction between PAA and wastewater constituents, such as chloride ion and iron species, needs to be considered. Chloride can react with PAA to form hypochlorous acid (HOCl; i.e., free chlorine; reaction 2),[29] thereby inducing damage to polyamide membranes. Iron species, either as dissolved/colloidal species or as iron oxide particulates/scales, can react with H_2O_2 present in commercial PAA products to generate hydroxyl radicals (•OH) via Fenton reaction (reactions 3–4).[31] The reaction between H_2O_2 and Fe has been shown to result in the loss of polyamide membrane performance.[17, 32] More importantly, ferrous iron (Fe(II)) can react with PAA to generate Fe(IV) and carbon-centered radicals that were shown to be much more reactive than •OH.[33] Although Fe(II) concentration is typically low in wastewater, the high oxidative reactivity of PAA/Fe(II) warrants examination.

$$CH_3COOOH + Cl^- = HOCl + CH_3COO^- + H_2O$$

(R2) $k = (1.47 \pm 0.58) \times 10^{-5}\ M^{-1}\ s^{-1}$ [29]

93 $Fe^{2+} + H_2O_2 = Fe^{3+} + \bullet OH + OH^-$ (R3) k = 63–76 M^{-1} s^{-1} [31]

94 $Fe^{3+} + H_2O_2 = Fe^{2+} + H^+ + HO_2\bullet$ (R4) k = 0.001–0.01 M^{-1} s^{-1} [31]

95 The overall goal of this work is to assess the performance stability of a commercial
96 polyamide nanofiltration membrane (NF90) upon exposure to PAA and free chlorine. The
97 specific objectives are to (1) compare the membrane performance of NF90 after exposure to
98 PAA with those exposed to sodium hypochlorite (NaOCl); (2) examine the effect of two
99 wastewater constituents, chloride and Fe(II), on membrane performance and characteristics
100 upon NaOCl and PAA exposure; (3) explore reaction mechanisms between polyamide and
101 PAA/NaOCl. The last objective was pursued via surface characterization techniques that can
102 detect changes in membrane surface functional groups, as well as oxidation experiments using
103 a model aromatic amide compound benzanilide.
104

105 ## 2 Materials and Methods

106 ### 2.1 Membrane and Chemicals

107 A commercial flat-sheet, fully aromatic polyamide nanofiltration membrane (NF90,
108 FilmTec™, Dow, Minneapolis, MN, USA) was used in this study. The PAA stock solution
109 (Sigma-Aldrich, St Louis, MO) contains 32% PAA and 5.4% H_2O_2 (PAA to H_2O_2 mass ratio
110 1:0.17, molar ratio 1:0.38). All chemicals were used as received. Text S1 provides further
111 details of the source and purity of the chemicals and a short summary of the composition of
112 typical commercial PAA products.

113 ### 2.2 Membrane Oxidant Exposure Experiments

114 As-received membrane sheets were hydrated in Milli-Q water for 24 h and washed three
115 times before use. After wash, circular membrane coupons (43 mm in diameter) were fully
116 immersed in glass Petri dishes containing 50 ml aqueous solutions of PAA, NaOCl, or H_2O_2
117 and sealed with parafilm. After a set period of time, membrane coupons were removed from

the oxidant solutions, rinsed with deionized water, and tested for performance in a dead-end filtration cell (section 2.3) or subjected to surface characterization (section 2.4). The membrane oxidant exposure protocol is adopted from previous studies of polyamide degradation by free chlorine[4, 5, 34, 35] or chloramine[36]. Although this protocol does not apply hydraulic pressure during oxidant exposure, rendering it not possible to capture the compounding effects of physical processes such as membrane compaction and oxidant diffusion,[37] it allows us to focus on the chemical reactions between polyamide and oxidants and to compare the PAA results with those from previous chlorine studies[4, 5, 34, 35] to assess the feasibility of PAA as a membrane disinfecting agent.

Relatively high initial oxidant concentrations (100 and 1000 mg L^{-1}) were used to allow observation of polyamide degradation within a reasonable experimental timeframe. These concentrations were selected to be within the range used in previous chlorine and H_2O_2 studies.[4, 5, 16, 17, 34, 38] Oxidant concentrations were monitored over the course of the experiments using methods described in Text S2 (example oxidant decay curves shown in Figures S1). The oxidant exposure was calculated using the product of concentration and contact time (i.e., C•t). To account for oxidant decay during the experiments, area under the oxidant concentration–time curves (e.g., Figure S1) was integrated using the midpoint Riemann sum (rectangle) rule. PAA decayed approximately 25% over 24 h (Figure S1a); therefore, PAA solutions were refreshed every 24 h during membrane exposure. NaOCl decayed relatively slowly (reaching 45% decay after 180 h), so the solutions were not refreshed, but the decay was taken into consideration in the calculation of exposure. H_2O_2 did not show appreciable decay over the course of the experiment (180 h). The initial pH of the oxidant solutions was adjusted to 6.5 using 2 N NaOH (for PAA) or 2 N HCl (for NaOCl). No pH adjustment was needed for H_2O_2. The oxidant solutions were not buffered to avoid de-swelling of the polymer network under the high ionic strength needed for the buffer capacity (Figure S2).[39-41] Over the course of the

experiments, the pH of the PAA solutions dropped slightly (< 0.9 pH unit) within the first 12 h and then leveled off (Figure S3); the pH of the NaOCl and H_2O_2 solutions remained stable.

When considering the effect of chloride, membrane coupons were exposed to solutions containing oxidant(s) and varying concentrations of sodium chloride (NaCl; 0, 300 and 1200 mg L^{-1} of Cl^-). Three oxidant combinations were evaluated: PAA (100 mg L^{-1}, with 17 mg L^{-1} H_2O_2 from the commercial stock), a mixture of PAA (100 mg L^{-1}) and H_2O_2 (217 mg L^{-1}), and NaOCl (100 mg L^{-1}). The mass ratio of H_2O_2 to PAA in the mixture represents the higher end of those found in commercial formulations.[21] Initial solution pH was adjusted to 6.5 using HCl or NaOH. Membrane performance was evaluated after 24 h of oxidant exposure. To study the effects of Fe(II) on oxidant-induced polyamide degradation, ferrous sulfate ($FeSO_4$; 0, 1, and 10 mg L^{-1} of Fe(II)) was added to the oxidant solutions for membrane exposure. The three oxidant combinations evaluated were the same as those for chloride experiments. The high Fe(II) concentrations were used to represent a challenging case, especially to capture the fast kinetics reported for PAA/Fe(II) systems.[33, 42]

2.3 Membrane Performance Test

The performance of pristine and oxidant-exposed membranes, including their pure water flux and rejection of salt (NaCl) and small organic compounds, was tested. After exposure to the oxidant solutions for a set period of time, the membrane coupons were removed from the glass Petri dishes, rinsed with Milli-Q water, and placed in a 70 mL polycarbonate dead-end stirred cell (UHP 43 70 mL Stirred Cell, Sterlitech Corporation, WA, USA). The stirring rate was set at ~700 rpm. The effective membrane area was 11.3 cm^2. The operating pressure was supplied by N_2 gas and set at 4 bar. Feed volume of 50 mL was used for both pure water flux and solute rejection tests. For pure water flux measurement, Milli-Q water was used as the feed; the permeate was collected on a balance, the weight change of which was recorded every 5 s. The pure water flux was recorded when a stable rate of weight change was obtained

(< 5% variation between two consecutive readings). Subsequently, the feed was switched to a 2000 mg L^{-1} NaCl solution for salt rejection measurement. The conductivity of every 10 mL permeate was measured using a conductivity meter (Vernier Software & Technology, OR, USA), and then the permeate was returned to the remaining feed in the cell. Permeate NaCl concentration was calculated based on the conductivity using a calibration curve. This process was repeated until a stable permeate conductivity was obtained (< 5% change between two measurements). Salt rejection and average salt flux were calculated using Equation 1 and 2, respectively. To measure the rejection of organic compounds, 5500 mg L^{-1} solutions of ethylene glycol (EG), glycerol, or polyethylene glycol 200 (PEG 200) were used as the feed. The first 10 mL permeate was returned to the cell to minimize the effect of adsorption and the permeate of the second run was collected for analysis. Both permeate and feed solutions were analyzed using a total organic carbon (TOC) analyzer (Shimadzu Corporation, Japan). The rejection and average flux were calculated using Equation 1 and 2, respectively.

$$R\ (\%) = \left(1 - \frac{C_p}{C_F}\right) \times 100 \qquad \text{(Equation 1)}$$

$$J_s = C_P \times J_w \qquad \text{(Equation 2)}$$

where R is the rejection of NaCl or organic compounds (%); C_P and C_F are the concentrations of NaCl or organic compounds (g L^{-1}) in the permeate and feed, respectively; J_s is the flux of NaCl or organic compounds (g m^{-2} h^{-1}); and J_w is the water flux (L m^{-2} h^{-1}) with solutions of NaCl or organic compounds as feed (i.e., not the pure water flux).

2.4 Membrane Surface Characterization

All membrane samples were rinsed with Milli-Q water and air-dried prior to surface characterization. Static water contact angle was determined by a goniometer (Model 190, Rame-Hart́ Instrument Co.) using a sessile drop method (5 μL) with Milli-Q water as the probing liquid. The reported water contact angle after PAA or NaOCl exposure was the average

of two independently exposed membranes, with 10 different locations measured for each membrane (i.e., a total of 20 measurements).

Spectra from Fourier-transform infrared spectroscopy (FTIR) were collected from a Perkin-Elmer Spectrum Two Spectrometer equipped with a diamond crystal attenuated total reflection accessory. Spectra were collected from 400–4000 cm^{-1} with 4 cm^{-1} resolution against an air background. In order to quantify the change in the abundance of free carboxylic acid functional group, the FTIR feature from 1600 to 1800 cm^{-1} (amide I) was deconvoluted with four fitted peaks to represent C=C aromatic ring vibration (1608 cm^{-1}), H-bonded amide C=O (1650 cm^{-1}), free amide C=O (1677 cm^{-1}), and free carboxylic acid C=O (1720 cm^{-1}). These peak positions have been developed and confirmed with density functional theory calculation and were applied to polyamide membrane analysis.[43] The fitting parameters (i.e., peak position, width at half maximum, and peak shape) were held constant when fitting for different samples. Peak fitting was performed with Peak Analyzer in OriginPro 8.1®. The ratio of the carboxylic acid C=O peak area to the sum of the peak areas for the two amide C=O groups (H-bonded C=O and free amide C=O) was calculated as an indicator of the amount of carboxylic acid group. Only the spectra of pristine and PAA-exposed membrane were processed, as the NaOCl-exposed membranes had a significant shift at the amide I region.

An X-ray photoelectron spectroscopy (XPS) instrument (PHI Versaprobe II) with a monochromated Al K-alpha X-ray source was used. The X-ray source has a spot size of 200 μm and beam power of 50 W at a vacuum pressure of 0.8×10^{-9} to 2×10^{-8} Torr with a take-off angle of 45 degrees. Survey spectra were first acquired using an analyzer pass energy of 187.8 eV with a step size of 0.8 eV, and high energy resolution spectra were then acquired using an analyzer pass energy of 23.5 eV with a step size of 0.1 eV.

Membrane surface roughness was determined using atomic force microscopy (AFM, Dimension Icon, Bruker Corporation, USA). Imaging was done in tapping mode using a Si

cantilever (TESPA-V2) with a spring constant of 42 N/m. After scanning, the images were corrected for curvature and slope, and the root-mean-squared roughness (R_{rms}) was calculated. For each membrane sample, scan areas of 10 μm × 10 μm were imaged at 5 different positions, and the average R_{rms} was reported. A field emission scanning electron microscope (FESEM, Hitachi S4000, Japan) was used to provide micrographs showing the surface morphology of the membranes.

2.5 Benzanilide Experiments and Analysis

Benzanilide is an aromatic amide that has been used as a model compound to investigate the reaction mechanisms between polyamide and free chlorine.[44] The primary goals of the benzanilide experiments are to examine the reactivity of PAA/Fe(II) mixture towards aromatic amide and to explore the oxygen functional group formed in PAA reactions that may not be captured by membrane surface characterization. Accordingly, most experiments were conducted at pH 3, where the reactivity of PAA or PAA/Fe(II) is enhanced. The initial benzanilide concentrations were within the range of 25–30 μM, allowing comparison between peroxide oxidants within a timescale comparable to the membrane exposure experiments.

Two sets of experiments were conducted. In the first set, high peroxide concentrations (1000–2000 mg L^{-1}; i.e., 13.2–64 mM) were used, and the solution conditions are summarized in Table S1. After benzanilide (stock solution 50.7 mM in acetonitrile) was spiked into 10 mL of PAA, H_2O_2, or PAA+H_2O_2 solutions, the solution pH was adjusted to pH 3 with H_2SO_4 (without buffer). For experiments with Fe(II) (10 mg L^{-1}; i.e., 0.179 mM), freshly prepared $FeSO_4$ stock solution was added after pH adjustment. A second set of experiments were conducted using lower concentrations of PAA (0.1 mM) and Fe(II) (0.1 mM), matching the conditions where high PAA/Fe(II) reactivity towards micropollutants was reported.[33] The solution conditions are summarized in Table S2. For this set of experiments, solutions containing benzanilide and $FeSO_4$ were pH adjusted to pH 3 (without buffer) and then spiked

with peroxides to initiate the reaction. Lastly, additional experiments at pH 6.5 were conducted for product analysis. All experiments were conducted at room temperature (23 ± 2 ºC).

After a set period of time, residual oxidants were quenched by sodium thiosulfate and the samples were processed immediately. Samples from the Fe(II) experiments were filtered by 0.45 μm glass fiber syringe filters after thiosulfate quenching to remove potential iron precipitates. Time zero samples were processed similarly as those from later time points (i.e., quenched, filtered, and analyzed as described below) to ensure that the fast initial kinetics,[33, 42] if present, would be captured. Samples were analyzed by high-performance liquid chromatography (HPLC) with a diode array detector for benzanilide concentrations (detection limit 0.5 μM). The analysis and exploration of benzanilide transformation products were conducted using a liquid chromatography - triple quadrupole mass spectrometer (LC-QQQ, Agilent 6470). Benzoic acid, a possible degradation product of benzanilide, was quantified against an authentic standard. Full scan of the mass spectra was employed to search for other possible oxidation products. Further details on the analytical methods are provided in Text S3.

3 Results and Discussion

3.1 Effects of PAA and NaOCl Exposure on Membrane Performance

As shown in Figure 1, PAA exposure had much less impact on the performance of NF90 membrane than NaOCl exposure. For membranes exposed to PAA, the pure water flux (Figure 1a) initially declined by 20%, from 34.6 to 26.7 L m^{-2} h^{-1}, as PAA exposure increased from 0 to 5.4 g h L^{-1}; however, as PAA exposure increased to 14.2 g h L^{-1}, the pure water flux recovered to the original value, and remained stable with PAA exposure up to 180 g h L^{-1}. In contrast, the pure water flux of NaOCl-exposed membranes decreased by 47%, from 34.6 to 18.4 L m^{-2} h^{-1}, after only 1.0 g h L^{-1} exposure. With NaOCl exposure between 2.0 and 24 g h L^{-1}, the membrane water flux remained low, ranging from 7.6 to 16.2 L m^{-2} h^{-1}. Further increase

in NaOCl exposure (up to 140 g h L^{-1}) increased the pure water flux, but this can be explained by polyamide damage, as supported by the change in salt rejection (Figure 1b) and surface chemistry (section 3.3) described below. The changes in membrane pure water flux as a function of NaOCl exposure observed in our experiments are consistent with previous findings.[4, 37, 45, 46] As a common component of commercial PAA formulation, H_2O_2 was examined for its compatibility with polyamide. Exposure of H_2O_2 at 180 g h L^{-1} exhibited negligible change in the pure water flux of NF90, consistent with the previously reported H_2O_2 tolerance for polyamide RO membranes (> 744 g h L^{-1}).[15, 16]

The salt (NaCl) rejection (Figure 1b) of PAA-exposed membranes increased from 77% to 92% as exposure increased from 0 to 14 g h L^{-1}, and remained constant with further increase in exposure up to 180 g h L^{-1}. For NaOCl-exposed membranes, NaCl rejection first increased sharply to 97% after 2 g h L^{-1} exposure, and then decreased at exposure past 24 g h L^{-1} to reach 65% at 140 g h L^{-1} exposure, indicating the loss of polyamide selectivity. H_2O_2 exposure of 180 g h L^{-1} did not affect NaCl rejection.

The effects of oxidant exposure on membrane performance were also evaluated with a lower initial PAA or NaOCl concentration (100 mg L^{-1}) (Figure S5). The change in pure water flux, NaCl rejection, and NaCl flux followed trends similar to those observed with the 1000 mg L^{-1} initial oxidant concentration. For PAA-exposed membranes, the pure water flux declined from 35 to 29 L m^{-2} h^{-1} as the exposure increased from 0 to 0.50 g h L^{-1} exposure, but then fully recovered at 0.97 g h L^{-1} exposure, and remained constant as exposure further increased to 2.2 g h L^{-1}.

For the ability of membranes to reject organic compounds, PAA exposure again exhibited much less effect than NaOCl (Figure 1c). The three organic compounds, ethylene glycol (EG), glycerol, and PEG 200, were used as models for the neutral, hydrophilic, and low molecular weight compounds in groups of trace organic contaminants such as pharmaceuticals,

industrial chemicals, and disinfection byproducts that are particularly problematic in wastewater potable reuse.[9, 47-49] For the smallest compound, EG (MW 62 g mol^{-1}), the rejection was almost unchanged after PAA exposure of 5.4 and 180 g h L^{-1} (26% and 32%, respectively) compared with the pristine membrane (33%). In contrast, the rejection of EG after NaOCl exposure drastically changed to 45% and 19% after 1 and 140 g h L^{-1} exposure, respectively. For glycerol (92 g mol^{-1}) and PEG 200 (200 g mol^{-1}), the rejection after PAA exposure (180 g h L^{-1}) was within 10% of that of the pristine membrane; whereas the rejection after 140 g h L^{-1} NaOCl exposure decreased dramatically (from 77% to 29% for glycerol and from 93% to 36% for PEG 200). The performance loss in rejecting organic compounds upon NaOCl exposure indicates severe damage to the polyamide active layer, consistent with the NaCl rejection results.

3.2 Effects of Chloride and Fe(II) on Oxidative Membrane Damage

To investigate the effects of the two common wastewater constituents chloride and Fe(II) on PAA/H_2O_2 chemistry and its reaction with polyamide, similar exposure tests were performed with a 24 h exposure time. Two chloride concentrations (300 and 1200 mg L^{-1}) covering the range of typical wastewater were tested (Figure 2a and 2b). Compared with membranes exposed to PAA alone (with small amount of H_2O_2, Table S3), the presence of chloride during PAA exposure resulted in only a slightly lower pure water flux (< 10% difference), and did not affect salt rejection. Similarly, chloride did not affect the performance of the membranes exposed to a mixture of PAA+H_2O_2 (mass ratio 1:2.17) or NaOCl. Although the reaction between PAA and chloride is known to form free chlorine (i.e., hypochlorous acid HOCl; reaction 2),[29] results from our membrane experiments suggest that the generation of HOCl was likely insufficient to cause measurable membrane damage. Indeed, using the second-order rate constant of reaction 2,[29] calculation shows that the amount of HOCl formed would be small (2.4–5.6 mg L^{-1} as Cl_2) after 24 h exposure to 100 mg L^{-1} PAA and 1200 mg

317 L^{-1} chloride. Similar calculation further predicts that HOCl generation (< 0.03 mg L^{-1} as Cl_2)
318 would be below the typical free chlorine tolerance level of polyamide membrane (e.g., 0.1 mg
319 L^{-1})[6] under conditions relevant to PAA disinfection for membrane pretreatment in wastewater
320 reuse systems (e.g., PAA dose of 1–6 mg L^{-1} and contact time of 0.5–2 h).[21] Furthermore, H_2O_2,
321 present in all commercial PAA products, is capable of quenching HOCl (reaction 5), and hence
322 is likely to further ameliorate any HOCl effect. The presence of H_2O_2 has been shown to
323 suppress the chlorination of organic compounds in mixtures of PAA and chloride.[29] The
324 reactive oxygen species singlet oxygen ($^1O_2$) has been reported as a product of reaction 5,[50] but
325 it was shown to be much less damaging to polyamide materials than free chlorine.[51] Overall,
326 our results suggest that the PAA-chloride reaction is not expected to exert a significant impact
327 on the PAA-polyamide compatibility. It should be noted that this conclusion only applies to
328 chloride levels relevant to wastewater; for high chloride feed streams (e.g., seawater),
329 significant damage to the polyamide membrane can occur (Text S4).

330 $HOCl + HO_2^- = Cl^- + {}^1O_2 + H_2O$ (R5) $k = 4.4 \times 10^7\ M^{-1}\ s^{-1}$ [50]

331 Regarding the effects of Fe(II), we initially hypothesized that Fe (II) would cause
332 additional damage to polyamide membranes during PAA exposure via two mechanisms: (1)
333 the reactive species generated by PAA/Fe(II) can degrade polyamide, based on the extremely
334 high oxidative reactivity of the PAA/Fe(II) mixture towards micropollutants reported
335 previously;[33, 42] (2) the •OH generated by the reaction between Fe(II) and the H_2O_2 present in
336 the PAA formulation (i.e., Fenton reaction) can also degrade polyamide membranes.[17, 32] Two
337 Fe(II) concentrations (1 and 10 mg L^{-1}) higher than those typically encountered in wastewater
338 were tested to present worst-case scenarios. Unexpectedly, the presence of Fe(II) during
339 membrane exposure to PAA, PAA+H_2O_2, or NaOCl did not exert additional impacts on the
340 membrane water flux compared with oxidant exposure alone (Figure 2c). NaCl rejection values
341 (Figure 2d) were not affected by the presence of Fe(II) during oxidant exposure; the only

exception was the membranes exposed to PAA+H_2O_2 in the presence of 10 mg L^{-1} Fe(II), which exhibited slightly lower NaCl rejection (83%) than those exposed to PAA+ H_2O_2 alone (89%). In the presence of Fe(II), PAA decayed rapidly (Figure S7) in a similar fashion as reported in the literature,[33] resulting in low PAA exposure in the 24 h experiments (Table S3). However, this does not invalidate the stability of polyamide membrane upon exposure to PAA/Fe(II), because the high reactivity of PAA/Fe(II) in degrading organic compounds was observed within the initial 10 min of the experiments.[33, 42] Previous studies also showed that when H_2O_2 alone was the oxidant, iron species, either generated from all-steel apparatus[32] or dosed as goethite, ferric oxide, or $FeSO_4$,[17] exhibited catalytic effect towards the deterioration of membrane performance, which was attributed to the •OH generated via Fenton reaction (reactions 3–4).[17, 32] Considering that H_2O_2 was present in all of our PAA experiments, these early findings contrast our observation that Fe(II) had little or no effect, even in the PAA+H_2O_2 mixture with high concentrations of Fe(II). This may be rationalized by the quenching of •OH by PAA, which is further discussed in section 3.4. Lastly, we did not observe catalytic effect of Fe(II) on NaOCl-induced polyamide degradation, which may be attributed to the relatively low NaOCl exposure in our experiments (< 1.8 g h L^{-1}). A measurable catalytic effect was previously shown for NaOCl exposure level > 4 g h L^{-1} [52] or in long-term (~300 h) pilot-scale testing[53].

3.3 Mechanism of Polyamide Degradation: Membrane Surface Characterization

The chemical changes on membrane surfaces induced by PAA or NaOCl were characterized using FTIR, XPS, contact angle measurement, and AFM. The results collectively showed that PAA induced less change to the polyamide membrane surface than NaOCl.

Figure 3a compares the FTIR spectra of the pristine membrane with those after exposure to PAA or NaOCl. The most prominent change in the FTIR spectra of the NaOCl-exposed membranes is the disappearance of the peaks at 1541 cm^{-1} (amide II band, N-H in-

plane bending) and 1609 cm^{-1} (N-H deformation vibration or C=C stretching vibration of aromatic rings), suggesting severe amide bond change at NaOCl exposure as low as 1 g h L^{-1}. This is consistent with the previous chlorine studies.[4, 37, 54] In contrast, such change was not observed in the FTIR spectrum of the membrane with PAA exposure up to 180 g h L^{-1}. In order to reveal potential PAA-polyamide reaction products, the spectra of PAA-exposed and pristine membranes were further analyzed to quantify carboxylic acid groups following a reported method.[43] The peak deconvolution for the amide I region of the FTIR spectra is shown in Figure 3b and 3c, with the peak fitting parameters summarized in Table 1. As an indicative of the relative content of carboxylic acids, the ratio of the carboxylic acid C=O peak area to the sum of the peak areas for the two amide C=O groups (H-bonded C=O and free amide C=O) (Table 1) increased from 0.130 for the pristine membrane to 0.149 for the PAA-exposed membrane, suggesting the generation of carboxylic acid groups from the cleavage of the amide bond. Furthermore, no other oxygen functional groups (e.g. hydroxyl group) were observed on the FTIR spectra.

XPS analysis (Table 2) corroborated the findings from FTIR. Both PAA and NaOCl increased oxygen functional groups on the membrane, as suggested by the change in O/N ratios, but the increase was smaller after PAA exposure than after NaOCl exposure. The O/N ratios of the pristine, PAA-exposed (180 g h L^{-1}), and NaOCl-exposed (140 g h L^{-1}) membranes were 1.02, 1.43, and 2.08, respectively. The new oxygen functional groups formed upon PAA exposure likely included carboxylic acid, as suggested by the FTIR analysis, but the formation of other oxygen-containing functional groups (e.g., hydroxyl group) cannot be excluded if their abundance was too low to be detected by FTIR (further discussion in section 3.4). In addition to serving as evidence of direct oxygen incorporation, the O/N ratio can also be used to estimate the degree of cross-linking in polyamide, with 1:1 ratio representing fully cross-linked polyamide layer and 2:1 ratio representing a linear polyamide.[55] Accordingly, our results

suggest that NaOCl resulted in a greater loss in polyamide cross-linking than PAA. The XPS results also suggest rapid chlorine incorporation into membranes during NaOCl exposure. The Cl/N ratio rapidly increased from 0 to 0.64 after 1 g h L^{-1} NaOCl exposure, and further increased to 0.98 after 140 g h L^{-1} exposure. This is consistent with the chlorine-polyamide reaction mechanism proposed in previous studies,[5, 56, 57] which involves facile *N*-chlorination on the amide bond followed by amide bond hydrolysis and/or ring chlorination via Orton rearrangement.

To uncover the changes induced by chloride and Fe(II) during PAA exposure that may not be captured by membrane performance tests, the membrane samples were examined by XPS (Table 1). The presence of 1200 mg L^{-1} chloride during PAA exposure (1.8 g h L^{-1}) introduced a small amount of chlorine (Cl/N 0.03) and enhanced oxygen incorporation (O/N ratio increased from 1.25 to 1.34), consistent with the estimate in section 3.2 that a small amount of HOCl was generated. The presence of Fe(II) during PAA exposure also led to a higher O/N ratio of 1.36 despite the low PAA exposure (0.26 g h L^{-1}), which may be attributed to the reactive species formed by PAA/H_2O_2/Fe(II) (further discussion in section 3.4).

Contact angle and surface roughness of the PAA- and NaOCl-exposed membranes were measured to provide additional surface characteristics with implications on both fouling potential and reaction mechanisms. PAA-exposed membranes have greater hydrophilicity and lower surface roughness than NaOCl-exposed membranes (Figure 4). The water contact angle of the membranes dropped from 63º to 46° after 180 g h L^{-1} PAA exposure (Figure 4a). In comparison, NaOCl exposure yielded an increase in the water contact angle to 76º at low exposure (1 g h L^{-1}) and then decreased to 58º with high exposure (140 g h L^{-1}). The changes in surface hydrophilicity is consistent with the formation of oxygen-containing functional groups such as carboxylic acids upon PAA exposure; in contrast, NaOCl exposure increased hydrophobicity as a result of *N*-chlorination, which is followed by amide bond cleavage that

results in an increase in hydrophilicity. PAA exposure did not result in a notable change in R_{rms}, but NaOCl exposure increased R_{rms} by 35% with exposure as low as 1 g h L^{-1} (Figure 4b). The latter is consistent with previous findings.[58, 59] The lower roughness and greater hydrophilicity of PAA-exposed membranes when compared with NaOCl-exposed membranes is promising, as these membrane characteristics are generally associated with lower fouling potential.[60-63] Future research is warranted to examine the fouling behavior of PAA-exposed membranes.

3.4 Reactions between Peroxides and Model Aromatic Amide Benzanilide

To complement surface characterization tools, the reactions between peroxides (PAA and H_2O_2) and benzanilide, a simple aromatic amide,[44] were examined for two purposes: (1) to verify the unexpected stability of aromatic amide upon exposure to PAA in the presence of Fe(II), as indicated by the membrane performance tests and (2) to explore the PAA-amide reaction products, especially with regard to the formation of oxygen functional groups that may not be captured by membrane surface characterization. Although different from polyamide molecules and network, benzanilide can provide molecular insights into the reaction mechanism that is challenging to be explored by other techniques.

3.4.1 Benzanilide Degradation by Peroxide Oxidants

To examine benzanilide reactivity in the presence of Fe(II) and PAA or H_2O_2, results from PAA or PAA+Fe(II) experiments were compared with those from experiments with additional H_2O_2 (i.e., PAA+H_2O_2+Fe(II)) or without PAA (i.e., H_2O_2+Fe(II)) (Table S1 and S2). Benzanilide degradation experiments were conducted at pH 3 in order to capture worst-case scenarios based on the following considerations: (1) the reported oxidative reactivity of PAA/Fe(II) towards micropollutants was higher at low pH, with rate constants increased by 3.5–10 times as pH decreased from 8.2 to 3;[33] (2) Fenton reaction (i.e., H_2O_2/Fe(II)) involving the H_2O_2 present in the PAA stock solution is favored at acidic pH, where precipitation of Fe(III) species is minimized;[64] (3) in the absence of Fe(II), the protonated form of PAA (pK_a

8.2 [65]) is a stronger oxidant (reduction potential 1.748 V vs. standard hydrogen electrode (SHE)) than its deprotonated form (1.005 V vs. SHE);[66] (4) PAA stability is higher (i.e., slower spontaneous decomposition and hydrolysis) at lower pH;[67] and (5) benzanilide does not have active acid-base functional groups affecting its reactivity between pH 3 and neutral pH.

Figure 5a shows the decay time profile of benzanilide with high initial concentrations of peroxides (13–64 mM), with the corresponding pseudo first-order rate constants shown in Table S6. Notably, PAA, H_2O_2, and PAA+Fe(II) degraded benzanilide similarly and slowly, reaching only 40% decay after 120 h. In comparison, H_2O_2+Fe(II) degraded benzanilide much more rapidly, achieving more than 98% decay within 6 h; the pseudo first-order decay rate constant increased by 1.6 times when H_2O_2 concentration doubled. Interestingly, the PAA+H_2O_2+Fe(II) solution exhibited intermediate reactivity, with a decay rate constant 10 times faster than that of PAA and PAA+Fe(II), but 10 times slower than that of H_2O_2+Fe(II). The reactivity of benzanilide found here supports the polyamide membrane performance after exposure to these oxidants (Figures 1 and 2). These results, however, contrast the extremely rapid degradation of micropollutants methylene blue, naproxen, and bisphenol-A by PAA/Fe(II).[33] To verify that our observation was not an artifact of the self-quenching of reactive intermediates by PAA, additional experiments were conducted using lower PAA (100 μM) and Fe(II) concentrations that matched those in the micropollutant study.[33] As shown in Figure 5b, benzanilide was stable in PAA solution over 24 h, and degraded by less than 10% in PAA+Fe(II) solution. In contrast, H_2O_2(38 μM)+Fe(II), containing the equivalent amount of H_2O_2 in PAA+Fe(II), degraded 25% of benzanilide within 1 h. H_2O_2(238 μM)+Fe(II), with 6 times higher concentration of H_2O_2, degraded 70% of benzanilide within 1 h. The mixture of PAA+H_2O_2(238 μM)+Fe(II) also degraded benzanilide rapidly, but at a slower rate than that of H_2O_2(238 μM)+Fe(II).

In summary, the results from the benzanilide experiments suggest that •OH generated by the H_2O_2/Fe(II) Fenton reactions is a major contributor to benzanilide degradation. The presence of PAA slowed down benzanilide degradation by H_2O_2/Fe(II), which may be attributed to the more rapid quenching of •OH by PAA than by H_2O_2[68, 69] and the rapid consumption of Fe(II) by PAA.[33] Such reactivity is unique to benzanilide and potentially polyamide, compared to the previously studied micropollutants such as methylene blue, naproxene, and bisphenol-A.[33, 42] We note that the reaction of other reactive species including Fe(IV) and carbon-centered radicals (e.g., acetylperoxyl radical) with benzanilide cannot be completely ruled out, especially since they have been reported to degrade micropollutants with aromatic and amide moieties, such as acetaminophen, sulfamethoxazole, and indomethacine.[70-72] Overall, the results of the benzanilide degradation experiments support the compatibility of polyamide membrane with PAA in the presence of iron, especially for PAA formulas using high PAA to H_2O_2 ratios.

3.4.2 Benzanilide Oxidation Products

The analysis of benzanilide oxidation products using LC-QQQ suggests that both amide bond breakage and ring oxidation occurred. Benzoic acid, a product from amide bond breakage, was detected in all PAA and H_2O_2 samples after reaction at pH 6.5 and pH 3 (Table S7), consistent with the detection of free carboxylic acids on polyamide membrane after PAA exposure by FTIR. However, the amount of benzoic acid formed accounted for only 1.8–17% of the amount of benzanilide degraded (Table S7), suggesting that there were other oxidation products. Three product peaks with an M/z ratio of 212 (i.e., 16 M/z higher than parent benzanilide; electrospray ionization in the negative ion mode) were detected in the pH 3 PAA 120 h samples (Table S8). Two of the peaks have retention times (15.1 and 17.0 min, respectively) longer than the parent benzanilide (14.4 min) on a gradient elution, while the third peak (14.1 min) elutes slightly earlier than benzanilide. We postulate that the faster eluting

peak represents a ring hydroxylation product that is more hydrophilic than the parent benzanilide, while the other two peaks represent two epoxide products. Peroxy acids are known to react with polycyclic aromatic hydrocarbons and form epoxide from alkenes.[73-75] These ring-oxidation products may be partially responsible for the oxygen incorporation of PAA-exposed membranes (XPS) and enhanced surface hydrophilicity (contact angle).

4 Conclusion

This study utilized multiple approaches, including membrane performance tests, surface characterization, and experiments with a model aromatic amide, to demonstrate the stability of NF90 polyamide membrane upon exposure to PAA. PAA exposure up to 180 g h L^{-1} resulted in less than 22% change in the pure water flux and salt (NaCl) rejection, and did not significantly influence the rejection of neutral hydrophilic organic compounds (MW 62–200 g mol^{-1}). In comparison, NaOCl induced severe change in pure water flux and NaCl rejection at much lower exposure. The change in membrane performance after PAA or NaOCl exposure was supported by membrane surface characterization. Results from FTIR, XPS, contact angle measurement, and AFM analyses collectively show that PAA induced much less chemical change to membrane surface than NaOCl. PAA exposure (180 g h L^{-1}) formed free carboxylic acid groups on the membrane, but the majority of the amide bond remained intact. In contrast, NaOCl severely altered the amide bonds in the polyamide network at exposure as low as 1 g h L^{-1}.

The presence of chloride and Fe(II) during PAA exposure did not accelerate the deterioration of membrane performance. Experiments using the model compound benzanilide confirmed that PAA/Fe(II) has a similar reactivity towards aromatic amide with PAA alone. The greater the H_2O_2 content in the PAA/Fe(II) mixture, the greater the reactivity. The H_2O_2/Fe(II) binary mixture had the highest reactivity. These results suggest that, rather than

damaging polyamide membranes, PAA may play a protective role by quenching the •OH generated from the H_2O_2/Fe(II) Fenton reactions. Thus we suggest that PAA formulas with a high PAA to H_2O_2 ratio are preferred for membrane disinfection when iron is concerned. Product analysis of benzanilide oxidation suggests that amide bond breakage (forming carboxylic acid) as well as ring oxidation (forming hydroxyl-substituted or epoxide products) are possible mechanisms for the reaction between PAA and aromatic amide, complementing the findings from FTIR and XPS analyses.

Overall, our results suggest that PAA can be a potential disinfectant with low impacts on the long-term performance of polyamide membranes for wastewater reuse in the presence of Fe(II) and chloride. Future research is warranted to continue exploring the reaction mechanisms between PAA and polyamide, to simultaneously examine membrane stability and fouling inhibition in cross-flow systems, and to consider other factors that would influence the implementation of PAA disinfection such as cost and residual management.

Acknowledgement

This research was partially supported by the National Science Foundation (#1652412) and the Bureau of Reclamation (R17AC00147). The authors thank Libby Shaw at MIT Center for Materials Science and Engineering for assisting with XPS analysis.

Competing Interests Statement

The authors have no competing interests to declare.

Reference:

1. J. R. Werber, C. O. Osuji and M. Elimelech, Materials for next-generation desalination and water purification membranes, *Nature Reviews Materials*, 2016, **1**.
2. D. M. Warsinger, S. Chakraborty, E. W. Tow, M. H. Plumlee, C. Bellona, S. Loutatidou, L. Karimi, A. M. Mikelonis, A. Achilli, A. Ghassemi, L. P. Padhye, S. A. Snyder, S. Curcio, C. D. Vecitis, H. A. Arafat and J. H. Lienhard, A review of polymeric membranes and processes for potable water reuse, *Progress in Polymer Science*, 2018, **81**, 209-237.
3. N. Misdan, W. J. Lau and A. F. Ismail, Seawater Reverse Osmosis (SWRO) desalination by thin-film composite membrane-Current development, challenges and future prospects, *Desalination*, 2012, **287**, 228-237.
4. V. T. Do, C. Y. Tang, M. Reinhard and J. O. Leckie, Degradation of Polyamide Nanofiltration and Reverse Osmosis Membranes by Hypochlorite, *Environmental Science & Technology*, 2012, **46**, 852-859.
5. V. T. Do, C. Y. Tang, M. Reinhard and J. O. Leckie, Effects of chlorine exposure conditions on physiochemical properties and performance of a polyamide membrane--mechanisms and implications, *Environ Sci Technol*, 2012, **46**, 13184-13192.
6. Dow Water & Process Solutions. FILMTEC™ Reverse Osmosis Membranes. Technical Manual, Form No.609-00071-1009 2011. 181 pp.
7. M. Dasilva, I. Tessaro and K. Wada, Investigation of oxidative degradation of polyamide reverse osmosis membranes by monochloramine solutions, *Journal of Membrane Science*, 2006, **282**, 375-382.
8. U.S. Environmental Protection Agency, Office of Water. Guidance Manual for Compliance with the Filtration and Disinfection Requirements for Public Water Systems Using Surface Water Sources. Washington, DC, 1989.
9. T. Zeng, M. J. Plewa and W. A. Mitch, N-Nitrosamines and halogenated disinfection byproducts in U.S. Full Advanced Treatment trains for potable reuse, *Water Res.*, 2016, **101**, 176-186.
10. S. S. Lau, X. Wei, K. Bokenkamp, E. D. Wagner, M. J. Plewa and W. A. Mitch, Assessing Additivity of Cytotoxicity Associated with Disinfection Byproducts in Potable Reuse and Conventional Drinking Waters, *Environmental Science & Technology*, 2020, **54**, 5729-5736.
11. T. Shintani, H. Matsuyama and N. Kurata, Development of a chlorine-resistant polyamide reverse osmosis membrane, *Desalination*, 2007, **207**, 340-348.
12. D. H. Shin, N. Kim and Y. T. Lee, Modification to the polyamide TFC RO membranes for improvement of chlorine-resistance, *Journal of Membrane Science*, 2011, **376**, 302-311.
13. S. Azari and L. Zou, Using zwitterionic amino acid l-DOPA to modify the surface of thin film composite polyamide reverse osmosis membranes to increase their fouling resistance, *J. Membrane Sci.*, 2012, **401-402**, 68-75.
14. E. M. Van Wagner, A. C. Sagle, M. M. Sharma, Y.-H. La and B. D. Freeman, Surface modification of commercial polyamide desalination membranes using poly(ethylene glycol) diglycidyl ether to enhance membrane fouling resistance, *J. Membrane Sci.*, 2011, **367**, 273-287.
15. R. Abejon, A. Garea and A. Irabien, Effective Lifetime Study of Commercial Reverse Osmosis Membranes for Optimal Hydrogen Peroxide Ultrapurification Processes, *Industrial & Engineering Chemistry Research*, 2013, **52**, 17270-17284.

16. R. Ling, L. Yu, T. P. T. Pham, J. H. Shao, J. P. Chen and M. Reinhard, The tolerance of a thin-film composite polyamide reverse osmosis membrane to hydrogen peroxide exposure, *Journal of Membrane Science*, 2017, **524**, 529-536.
17. L. Yu, R. Ling, J. P. Chen and M. Reinhard, Quantitative assessment of the iron-catalyzed degradation of a polyamide nanofiltration membrane by hydrogen peroxide, *Journal of Membrane Science*, 2019, **588**, 117154.
18. M. Kitis, Disinfection of wastewater with peracetic acid: a review, *Environment International*, 2004, **30**, 47-55.
19. J. Yu, Y. Baek, H. Yoon and J. Yoon, New disinfectant to control biofouling of polyamide reverse osmosis membrane, *Journal of Membrane Science*, 2013, **427**, 30-36.
20. J. Yu, G.-A. Shin, B. S. Oh, J.-I. Kye and J. Yoon, N-chlorosuccinimide as a novel agent for biofouling control in the polyamide reverse osmosis membrane process, *Desalination*, 2015, **357**, 1-7.
21. Water Environment Association of Texas, Peracetic Acid for Disinfection of Municipal Wastewater Effluent, 2017. ftp.weat.org/Presentations/2017_Peracetic_Acid_Slides.pdf Accessed Oct. 1, 2020
22. A. H. Hassaballah, T. Bhatt, J. Nyitrai, N. Dai and L. Sassoubre, Inactivation of E. coli, Enterococcus spp., somatic coliphage, and Cryptosporidium parvum in wastewater by peracetic acid (PAA), sodium hypochlorite, and combined PAA-ultraviolet disinfection, *Environmental Science: Water Research & Technology*, 2020, **6**, 197-209.
23. A. H. Hassaballah, J. Nyitrai, C. H. Hart, N. Dai and L. M. Sassoubre, A pilot-scale study of peracetic acid and ultraviolet light for wastewater disinfection, *Environmental Science: Water Research & Technology*, 2019, **5**, 1453-1463.
24. E. Veschetti, D. Cutilli, L. Bonadonna, R. Briancesco, C. Martini, G. Cecchini, P. Anastasi and M. Ottaviani, Pilot-plant comparative study of peracetic acid and sodium hypochlorite wastewater disinfection, *Water Research*, 2003, **37**, 78-94.
25. J. Koivunen and H. Heinonen-Tanski, Inactivation of enteric microorganisms with chemical disinfectants, UV irradiation and combined chemical/UV treatments, *Water Research*, 2005, **39**, 1519-1526.
26. K. Toté, T. Horemans, D. V. Berghe, L. Maes and P. Cos, Inhibitory Effect of Biocides on the Viable Masses and Matrices of Staphylococcus aureus and Pseudomonas aeruginosa Biofilms, *Applied and Environmental Microbiology*, 2010, **76**, 3135.
27. C. Zhang, P. J. B. Brown, R. J. Miles, T. A. White, D. G. Grant, D. Stalla and Z. Hu, Inhibition of regrowth of planktonic and biofilm bacteria after peracetic acid disinfection, *Water Research*, 2019, **149**, 640-649.
28. L. Domínguez Henao, A. Turolla and M. Antonelli, Disinfection by-products formation and ecotoxicological effects of effluents treated with peracetic acid: A review, *Chemosphere*, 2018, **213**, 25-40.
29. A. D. Shah, Z. Q. Liu, E. Salhi, T. Hofer and U. von Gunten, Peracetic acid oxidation of saline waters in the absence and presence of H_2O_2: secondary oxidant and disinfection byproduct formation, *Environ Sci Technol*, 2015, **49**, 1698-1705.
30. W. B. P. van den Broek, M. J. Boorsma, H. Huiting, M. G. Dusamos and S. van Agtmaal, Prevention of Biofouling in Industrial RO Systems: Experiences with Peracetic Acid, *Water Practice and Technology*, 2010, **5**.
31. A. D. Bokare and W. Choi, Review of iron-free Fenton-like systems for activating H2O2 in advanced oxidation processes, *Journal of Hazardous Materials*, 2014, **275**, 121-135.

32. R. Ling, L. Yu, T. P. T. Pham, J. Shao, J. P. Chen and M. Reinhard, Catalytic effect of iron on the tolerance of thin-film composite polyamide reverse osmosis membranes to hydrogen peroxide, *Journal of Membrane Science*, 2018, **548**, 91-98.
33. J. Kim, T. Zhang, W. Liu, P. Du, J. T. Dobson and C.-H. Huang, Advanced Oxidation Process with Peracetic Acid and Fe(II) for Contaminant Degradation, *Environmental Science & Technology*, 2019, **53**, 13312-13322.
34. A. Ettori, E. Gaudichet-Maurin, J. C. Schrotter, P. Aimar and C. Causserand, Permeability and chemical analysis of aromatic polyamide based membranes exposed to sodium hypochlorite, *Journal of Membrane Science*, 2011, **375**, 220-230.
35. Y.-N. Kwon, S. Hong, H. Choi and T. Tak, Surface modification of a polyamide reverse osmosis membrane for chlorine resistance improvement, *Journal of Membrane Science*, 2012, **415-416**, 192-198.
36. M. J. Cran, S. W. Bigger and S. R. Gray, Degradation of polyamide reverse osmosis membranes in the presence of chloramine, *Desalination*, 2011, **283**, 58-63.
37. J. E. Gu, B. M. Jun and Y. N. Kwon, Effect of chlorination condition and permeability of chlorine species on the chlorination of a polyamide membrane, *Water Res*, 2012, **46**, 5389-5400.
38. Y. Kwon and J. Leckie, Hypochlorite degradation of crosslinked polyamide membranesII. Changes in hydrogen bonding behavior and performance, *Journal of Membrane Science*, 2006, **282**, 456-464.
39. A. Braghetta, F. A. DiGiano and W. P. Ball, Nanofiltration of Natural Organic Matter: pH and Ionic Strength Effects, *Journal of Environmental Engineering*, 1997, **123**, 628-641.
40. V. Freger, Swelling and morphology of the skin layer of polyamide composite membranes: an atomic force microscopy study, *Environ. Sci. Technol.*, 2004, **38**, 3168-3175.
41. A. Escoda, P. Fievet, S. Lakard, A. Szymczyk and S. Déon, Influence of salts on the rejection of polyethyleneglycol by an NF organic membrane: Pore swelling and salting-out effects, *J. Membrane Sci.*, 2010, **347**, 174-182.
42. T. Luukkonen, T. Heyninck, J. Rämö and U. Lassi, Comparison of organic peracids in wastewater treatment: Disinfection, oxidation and corrosion, *Water Research*, 2015, **85**, 275-285.
43. T. J. Zimudzi, K. E. Feldman, J. F. Sturnfield, A. Roy, M. A. Hickner and C. M. Stafford, Quantifying Carboxylic Acid Concentration in Model Polyamide Desalination Membranes via Fourier Transform Infrared Spectroscopy, *Macromolecules*, 2018, **51**, 6623-6629.
44. K. Huang, K. P. Reber, M. D. Toomey, H. Haflich, J. A. Howarter and A. D. Shah, Reactivity of the Polyamide Membrane Monomer with Free Chlorine: Reaction Kinetics, Mechanisms, and the Role of Chloride, *Environmental Science & Technology*, 2019, **53**, 8167-8176.
45. S. Hong, I.-C. Kim, T. Tak and Y.-N. Kwon, Interfacially synthesized chlorine-resistant polyimide thin film composite (TFC) reverse osmosis (RO) membranes, *Desalination*, 2013, **309**, 18-26.
46. H. Li, P. Yu, H. G. Li and Y. B. Luo, The Chlorination and Chlorine Resistance Modification of Composite Polyamide Membrane, *Journal of Applied Polymer Science*, 2015, **132**.
47. L. N. Breitner, K. J. Howe and D. Minakata, Effect of Functional Chemistry on the Rejection of Low-Molecular Weight Neutral Organics through Reverse Osmosis Membranes for Potable Reuse, *Environmental Science & Technology*, 2019, **53**, 11401-11409.

48. C. Bellona, J. E. Drewes, P. Xu and G. Amy, Factors affecting the rejection of organic solutes during NF/RO treatment—a literature review, *Water Research*, 2004, **38**, 2795-2809.
49. J. Xu, T. N. Tran, H. Lin and N. Dai, Removal of disinfection byproducts in forward osmosis for wastewater recycling, *Journal of Membrane Science*, 2018, **564**, 352-360.
50. A. M. Held, D. J. Halko and J. K. Hurst, Mechanisms of chlorine oxidation of hydrogen peroxide, *Journal of the American Chemical Society*, 1978, **100**, 5732-5740.
51. N. Dam and P. R. Ogilby, On the Mechanism of Polyamide Degradation in Chlorinated Water, *Helvetica Chimica Acta*, 2001, **84**, 2540-2549.
52. R. Ling, J. Shao, J. P. Chen and M. Reinhard, Iron catalyzed degradation of an aromatic polyamide reverse osmosis membrane by free chlorine, *Journal of Membrane Science*, 2019, **577**, 205-211.
53. C. J. Gabelich, J. C. Frankin, F. W. Gerringer, K. P. Ishida and I. H. Suffet, Enhanced oxidation of polyamide membranes using monochloramine and ferrous iron, *Journal of Membrane Science*, 2005, **258**, 64-70.
54. C. Y. Tang, Y.-N. Kwon and J. O. Leckie, Effect of membrane chemistry and coating layer on physiochemical properties of thin film composite polyamide RO and NF membranes: I. FTIR and XPS characterization of polyamide and coating layer chemistry, *Desalination*, 2009, **242**, 149-167.
55. R. Verbeke, V. Gómez and I. F. J. Vankelecom, Chlorine-resistance of reverse osmosis (RO) polyamide membranes, *Progress in Polymer Science*, 2017, **72**, 1-15.
56. J. Xu, Z. Wang, X. Wei, S. Yang, J. Wang and S. Wang, The chlorination process of crosslinked aromatic polyamide reverse osmosis membrane: New insights from the study of self-made membrane, *Desalination*, 2013, **313**, 145-155.
57. J. Powell, J. Luh and O. Coronell, Amide Link Scission in the Polyamide Active Layers of Thin-Film Composite Membranes upon Exposure to Free Chlorine: Kinetics and Mechanisms, *Environ. Sci. Technol.*, 2015, **49**, 12136-12144.
58. H. H. Rana, N. K. Saha, S. K. Jewrajka and A. V. R. Reddy, Low fouling and improved chlorine resistant thin film composite reverse osmosis membranes by cerium(IV)/polyvinyl alcohol mediated surface modification, *Desalination*, 2015, **357**, 93-103.
59. B. C. Donose, S. Sukumar, M. Pidou, Y. Poussade, J. Keller and W. Gernjak, Effect of pH on the ageing of reverse osmosis membranes upon exposure to hypochlorite, *Desalination*, 2013, **309**, 97-105.
60. S. H. Maruf, L. Wang, A. R. Greenberg, J. Pellegrino and Y. Ding, Use of nanoimprinted surface patterns to mitigate colloidal deposition on ultrafiltration membranes, *Journal of Membrane Science*, 2013, **428**, 598-607.
61. M. Elimelech, Z. Xiaohua, A. E. Childress and H. Seungkwan, Role of membrane surface morphology in colloidal fouling of cellulose acetate and composite aromatic polyamide reverse osmosis membranes, *Journal of Membrane Science*, 1997, **127**, 101-109.
62. T. Tran, X. Chen, S. Doshi, C. M. Stafford and H. Lin, Grafting polysiloxane onto ultrafiltration membranes to optimize surface energy and mitigate fouling, *Soft Matter*, 2020, **16**, 5044-5053.
63. N. Shahkaramipour, A. Jafari, T. Tran, C. M. Stafford, C. Cheng and H. Lin, Maximizing the grafting of zwitterions onto the surface of ultrafiltration membranes to improve antifouling properties, *Journal of Membrane Science*, 2020, **601**, 117909.
64. A. Babuponnusami and K. Muthukumar, A review on Fenton and improvements to the Fenton process for wastewater treatment, *Journal of Environmental Chemical Engineering*, 2014, **2**, 557-572.

65. National Center for Biotechnology Information. PubChem Compound Summary for CID 6585, Peracetic acid. https://pubchem.ncbi.nlm.nih.gov/compound/Peracetic-acid. Accessed Oct. 5, 2020.
66. C. Zhang, P. J. B. Brown and Z. Hu, Thermodynamic properties of an emerging chemical disinfectant, peracetic acid, *Science of The Total Environment*, 2018, **621**, 948-959.
67. Z. Yuan, Y. Ni and A. R. P. Van Heiningen, Kinetics of the peracetic acid decomposition: Part II: pH effect and alkaline hydrolysis, *The Canadian Journal of Chemical Engineering*, 1997, **75**, 42-47.
68. M. Cai, P. Sun, L. Zhang and C.-H. Huang, UV/Peracetic Acid for Degradation of Pharmaceuticals and Reactive Species Evaluation, *Environmental Science & Technology*, 2017, **51**, 14217-14224.
69. T. Zhang and C.-H. Huang, Modeling the Kinetics of UV/Peracetic Acid Advanced Oxidation Process, *Environmental Science & Technology*, 2020, **54**, 7579-7590.
70. J. Kim, P. Du, W. Liu, C. Luo, H. Zhao and C.-H. Huang, Cobalt/Peracetic Acid: Advanced Oxidation of Aromatic Organic Compounds by Acetylperoxyl Radicals, *Environmental Science & Technology*, 2020, **54**, 5268-5278.
71. Z. Wang, J. Wang, B. Xiong, F. Bai, S. Wang, Y. Wan, L. Zhang, P. Xie and M. R. Wiesner, Application of Cobalt/Peracetic Acid to Degrade Sulfamethoxazole at Neutral Condition: Efficiency and Mechanisms, *Environmental Science & Technology*, 2020, **54**, 464-475.
72. H. Chen, T. Lin, W. Chen, H. Xu and H. Tao, Significant role of high-valent iron-oxo species in the degradation and detoxification of indomethacine, *Chemosphere*, 2020, **251**, 126451.
73. J. M. Shoulder, N. S. Alderman, C. M. Breneman and M. C. Nyman, Polycyclic aromatic hydrocarbon reaction rates with peroxy-acid treatment: prediction of reactivity using local ionization potential, *SAR and QSAR in Environmental Research*, 2013, **24**, 611-624.
74. R. D. Bach, C. Canepa, J. E. Winter and P. E. Blanchette, Mechanism of Acid-Catalyzed Epoxidation of Alkenes with Peroxy Acids, *The Journal of Organic Chemistry*, 1997, **62**, 5191-5197.
75. J. Kim and C.-H. Huang, Reactivity of Peracetic Acid with Organic Compounds: A Critical Review, *ACS ES&T Water*, 2020, DOI: 10.1021/acsestwater.0c00029.

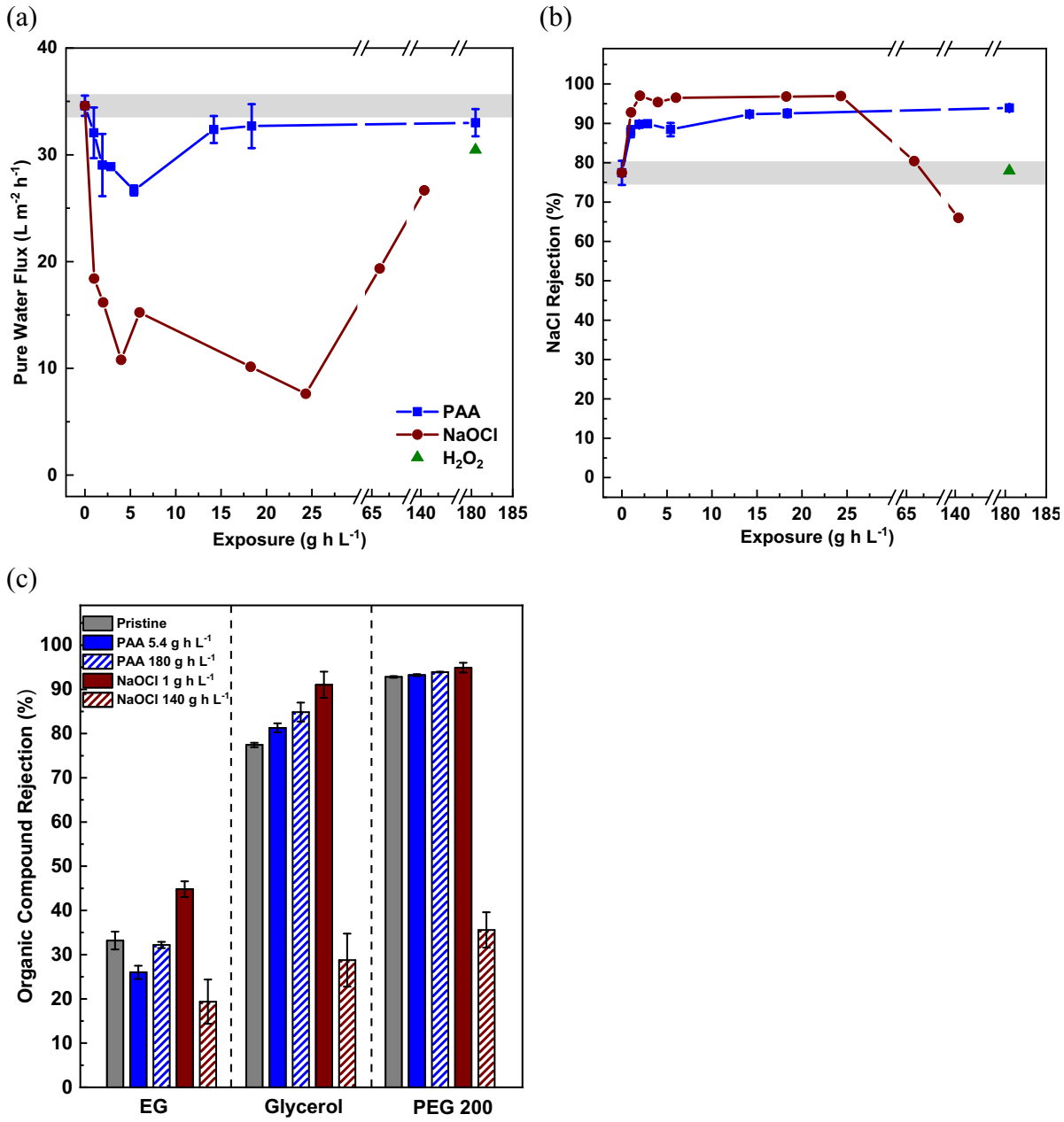

Figure 1. Comparison of (a) pure water flux, (b) NaCl rejection, and (c) organic compound rejection among pristine and oxidant-exposed NF90 membranes. Initial oxidant concentration was 1000 mg L^{-1}; the initial pH was 6.5. Performance tests were conducted under 4 bar pressure; further details are provided in sections 2.2 and 2.3. The PAA exposure experiments were conducted in duplicates, with error bars showing the difference between two replicate exposure experiments; when error bars are not visible, they fall within the symbols. The grey area in (a) and (b) represents the range of values for pristine membranes from duplicate tests. The three organic compounds ethylene glycol (EG), glycerol, polyethylene glycol 200 (PEG 200) have molecular weight of 62, 92, and 200 g mol^{-1}, respectively. The fluxes of NaCl and organic compounds corresponding to (b) and (c) are shown in Figure S4.

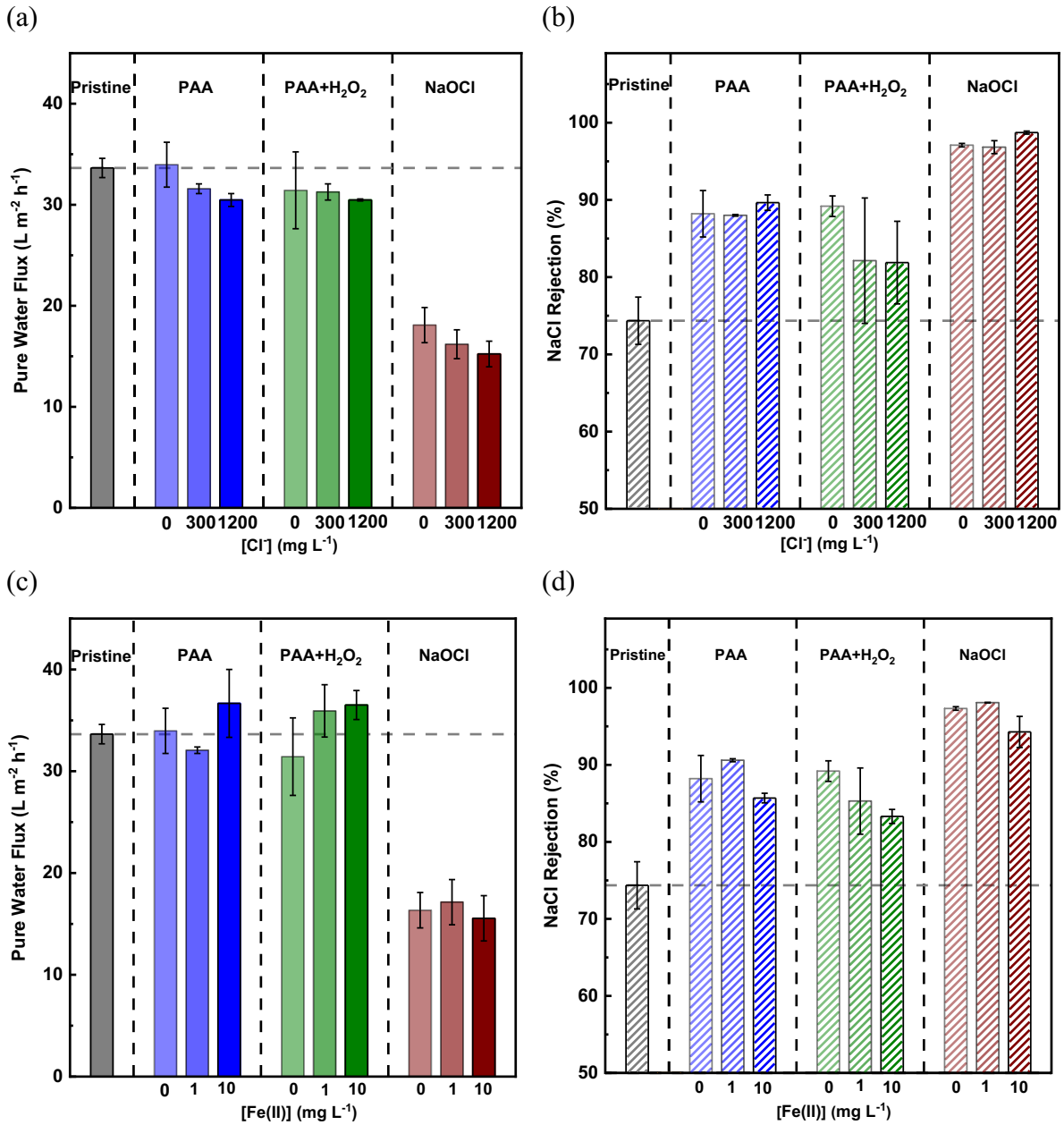

Figure 2. Effects of the presence of chloride ion (Cl^-) and Fe(II) during oxidant exposure on membrane performance. (a) and (b) show the pure water flux and NaCl rejection for membranes exposed to oxidants in the presence of varying concentrations of chloride. (c) and (d) are the corresponding graphs for membranes exposed to oxidants in the presence of Fe(II). Fe(II) was added as $FeSO_4$. Exposure time was 24 h; the initial oxidant concentrations were 100 mg L^{-1} PAA (containing 17 mg L^{-1} H_2O_2 from the commercial stock), 100 mg L^{-1} PAA and 217 mg L^{-1} H_2O_2, or 100 mg L^{-1} NaOCl. Detailed experimental conditions are described in sections 2.2 and 2.3. The PAA exposure values calculated based on the PAA decay profiles in the presence of chloride or Fe(II) are shown in Table S3. Error bars show the difference between two replicate exposure experiments.

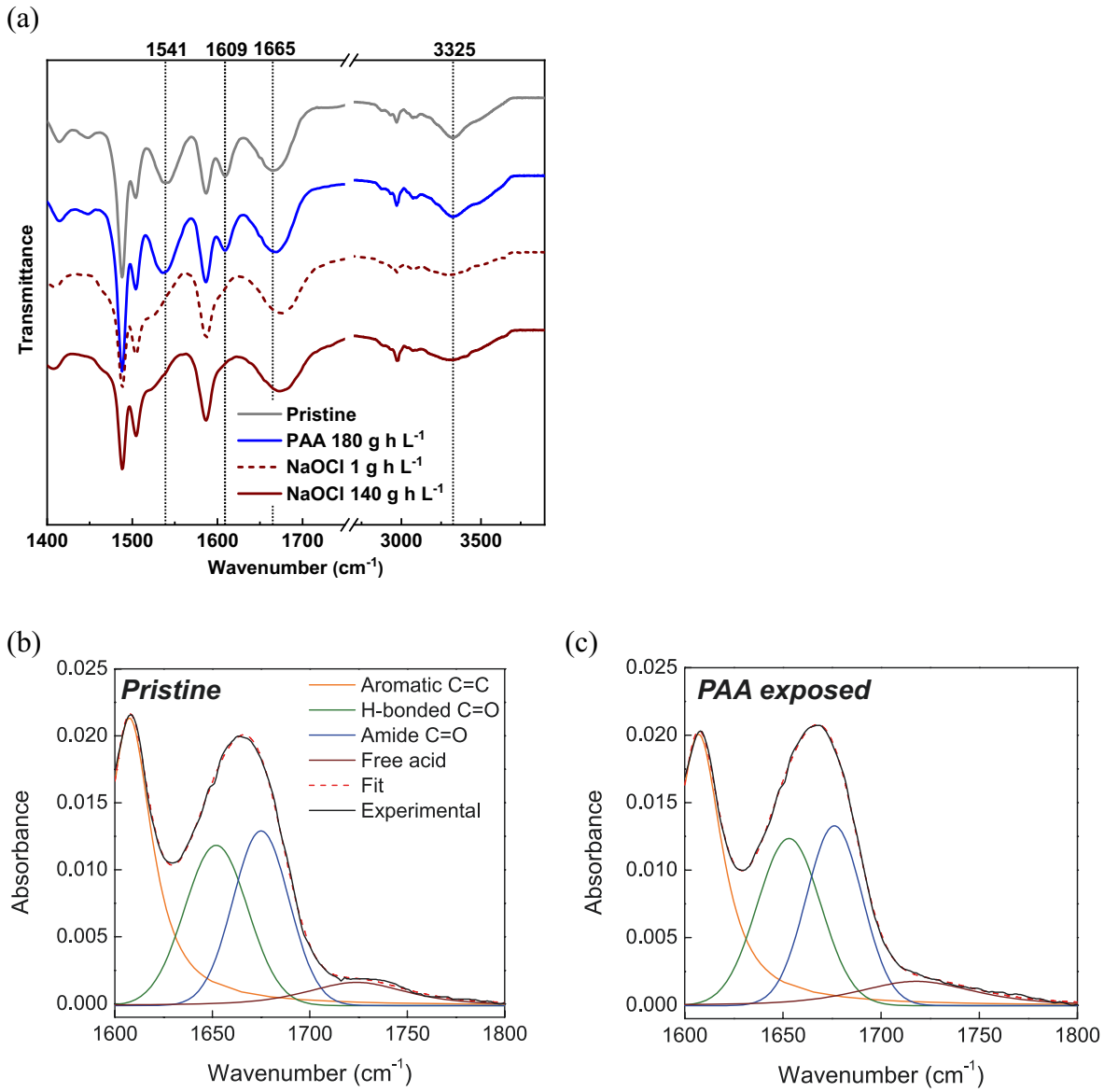

Figure 3. (a) FTIR spectra of pristine, PAA-exposed, and NaOCl-exposed NF90 membranes. Deconvoluted fits of amide I region of the FTIR spectra of (b) pristine and (c) PAA-exposed (180 g h L^{-1}) membranes. The initial oxidant concentration was 1000 mg L^{-1}; the initial solution pH was 6.5; room temperature. Other experimental conditions are as described in sections 2.2 and 2.3. The area of fitted peak at around 1720 cm^{-1} was used to calculate free carboxylic acid concentration. The ratio of carboxylic acid peak area over the summation of two amide C=O groups, H-bonded C=O (green) and amide C=O (blue), is calculated as an approximate of carboxylic acid group generation. The fitting and calculation details are presented in Table 2.

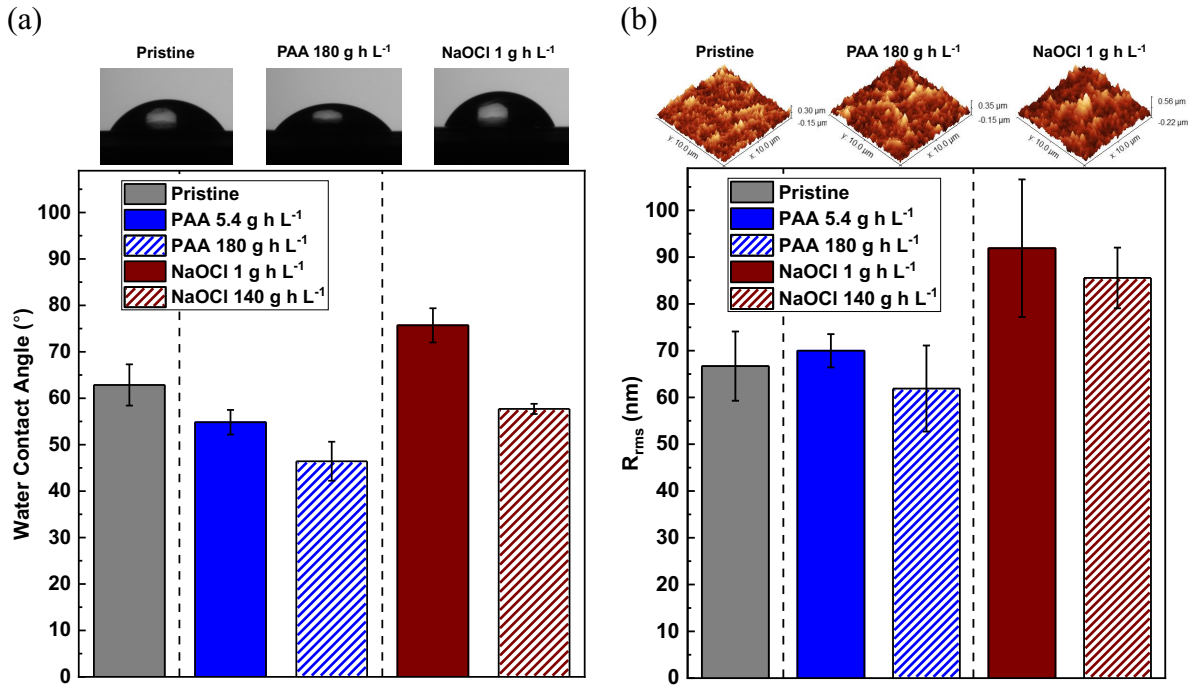

Figure 4. (a) Water contact angle and (b) root-mean-square roughness of pristine, PAA-exposed, and NaOCl-exposed NF90 membranes. The initial oxidant concentration was 1000 mg L^{-1}; the initial solution pH was 6.5; room temperature. Other experimental conditions are as described in sections 2.2 and 2.3. Water contact angle error bars represent the standard deviation of 20 measurements (2 membrane samples with 10 different locations measured for each). R_{rms} error bars represent standard deviation of measurements at 5 different locations on a membrane coupon. The AFM images are also shown in Figure S8.

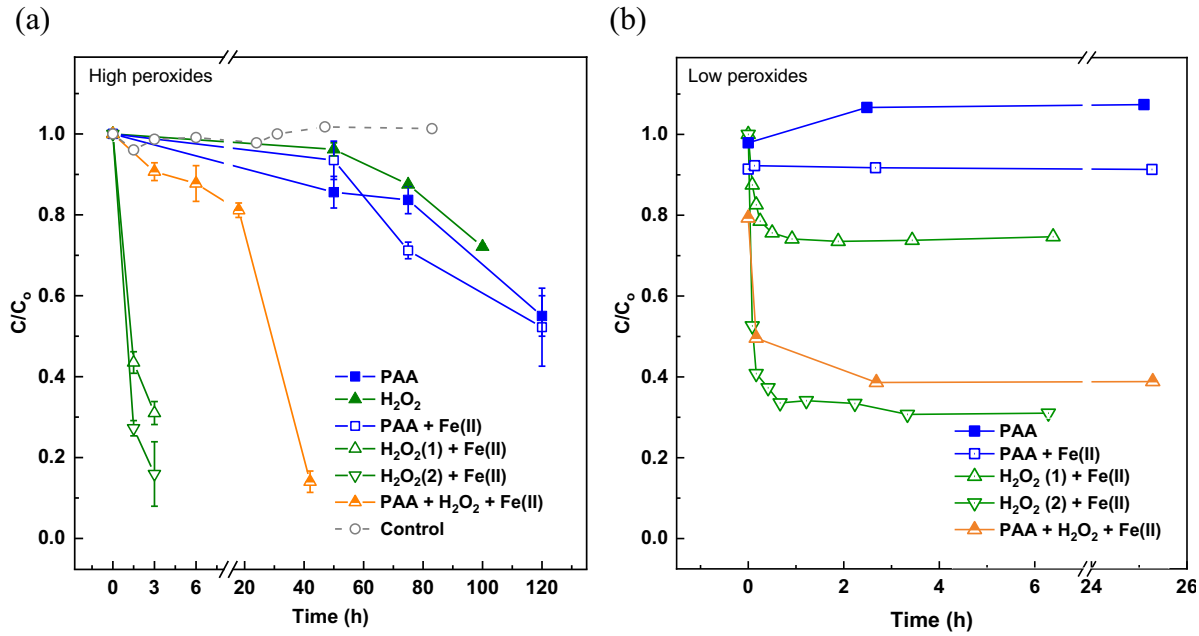

Figure 5. Benzanilide degradation at pH 3 with (a) high (13 to 64 mM, i.e., 1000–2000 mg L^{-1}) and (b) low initial (100 µM for PAA and 38 or 238 µM for H_2O_2) peroxide concentrations. The solution conditions are summarized in Table S1 and S2. The high initial peroxide concentrations match those in the membrane exposure experiments. The low initial peroxide concentrations simulate those used in reference [34] on micropollutants degradation by PAA/Fe(II). The control sample had no peroxide added. Residual oxidants were quenched by sodium thiosulfate. Samples from Fe(II) experiments were filtered using 0.45 µm glass fiber syringe filters prior to HPLC analysis. The concentration data for (a) and (b) are shown in Table S4 and S5, respectively. The pseudo first-order rate constants for (a) are shown in Table S6.

829 **Table 1.** Peak fitting parameters for the amide I region of the FTIR spectra of pristine and
830 PAA-exposed membranes and the comparison of their surface carboxylic acid content.

Sample	Component	Component peak shape	Peak center position (cm^{-1})	Full width at half maximum (cm^{-1})	Fitted peak area in fitting range (abs $\times cm^{-1}$)	Fit root mean square error	Ratio[a]
Pristine	C=C aromatic	92%Lorentze +Guassian	1607.5	27.5	0.57	1.75×10^{-4}	0.130
	H-bonded C=O	Gaussian	1652.0	38.1	0.49		
	C=O amide	Gaussian	1675.0	33.8	0.47		
	C=O acid	66%Lorentze +Guassian	1724.0	60.9	0.12		
PAA-exposed (180 g h L^{-1})	C=C aromatic	92%Lorentze +Guassian	1607.1	28.6	0.55	1.49×10^{-4}	0.149
	H-bonded C=O	Gaussian	1653.1	38.0	0.50		
	C=O amide	Gaussian	1676.2	33.5	0.48		
	C=O acid	66%Lorentze +Guassian	1718.0	70.0	0.15		

831 [a] Ratio of the area of the C=O acid peak to the sum of the area of the H-bonded C=O and C=O amide peaks
832
833

Table 2. Surface elemental composition of pristine and oxidant-exposed membranes determined by XPS analysis.

Oxidant Exposure[a]		Atomic Composition					
		C (%)	N (%)	O (%)	Cl (%)	O/N ratio	Cl/N ratio
Pristine	–	75.02	12.35	12.63	ND[b]	1.02	ND
PAA	5.4 g h L^{-1}	73.79	11.65	14.56	ND	1.25	ND
	180 g h L^{-1}	72.21	11.45	16.35	ND	1.43	ND
NaOCl	1 g h L^{-1}	69.51	10.18	13.83	6.49	1.36	0.64
	140 g h L^{-1}	70.10	7.36	15.32	7.23	2.08	0.98
PAA+Cl^-	1.80 g h L^{-1} [c]	74.02	11.0	14.69	0.29	1.34	0.03
PAA+Fe(II)	0.29 g h L^{-1}	72.18	11.35	15.42[d]	ND	1.36	ND

[a] The initial concentration of PAA or NaOCl was 1000 mg L^{-1} in experiments without Cl^- or Fe(II). For PAA+Fe and PAA+Cl experiments: the initial PAA concentration was 100 ppm; Fe(II) concentration was 10 mg L^{-1} (added as $FeSO_4$); Cl^- concentration was 1200 mg L^{-1}; exposure time was 24 h. The initial solution pH was 6.5. Room temperature. The exposure was calculated after accounting for oxidant decay.

[b] ND: not detected in a survey scan (detailed information provided section 2.4).

[c] Exposure calculated based on total oxidant concentration as PAA and HOCl cannot be differentiated by the DPD method.

[d] The oxygen content was corrected by subtracting the oxygen groups from Fe_2O_3 (0.7% Fe). Fe_2O_3 was confirmed by high-resolution XPS scan at 740–705 eV region.